DNA Binding Thermodynamics and Sequence Specificity of Chiral Piperazinecarbonyloxyalkyl Derivatives of Anthracene and Pyrene

Hans-Christian Becker* and Bengt Nordén

Contribution from the Department of Physical Chemistry, Chalmers University of Technology, S-412 96 Gothenburg, Sweden

Received February 7, 2000

Abstract: In this paper we report the DNA binding properties of piperazinecarbonyloxy-2-propyl derivatives of anthracene (**2**), pyrene (**3**), and phenylanthracene (**4**). An intercalative binding mode is found for **2** and **3**, while the phenyl group of **4** prevents intercalation and leads to external binding. Preferential binding of the (*S*)-enantiomers is found for both anthracene **2** and pyrene **3**. However, the enantiomeric preference is small, with $K_{(R)}/K_{(S)}$ being around 0.5 for both the anthracene and the pyrene compounds. This is interpreted in terms of orientation polarity in the binding, by which any intrinsic enantioselectivity is canceled by averaging of opposite binding orientations. The affinities for poly(dA-dT)$_2$ (AT) are 10^4 M^{-1} for anthracene derivative **2**, and 5×10^5 M^{-1} for pyrene derivative **2**. The affinities for poly(dG-dC)$_2$ (GC) are 1 order of magnitude lower than those for AT. This is explained by steric interference of the piperazinium tail with the exocyclic amino groups of guanine in the minor groove of GC, leading to a more shallow intercalation in GC than in AT, as also indicated by significantly less negative reduced linear dichroism of the intercalator absorption bands in the GC complexes. This behavior is consistent with that observed for the previously studied achiral analogues.[1] Binding thermodynamics support the difference in binding mode between AT and GC. The binding enthalpy of the AT complexes is significantly more negative than that of the corresponding GC complexes. This indicates a larger overlap of intercalating moiety and nucleobases in the AT complexes, consistent with the linear dichroism results.

Introduction

Ionic derivatives of amino-substituted polycyclic aromatic hydrocarbons, such as 9-anthrylmethylammonium chloride, are known to bind by intercalation into DNA without showing any significant sequence specificity.[2−4] Preferential intercalation into AT-rich regions of DNA has been observed for certain spatially more demanding alkylammonium compounds, attributed to steric repulsion between the alkylammonium tail and the exocyclic amino group of guanine in the minor groove of GC segments of DNA.[1,5−8] So far most investigations of binding properties of alkylammonium-substituted aromatic hydrocarbons have only been on achiral or racemic compounds.[2,6,7,9−11] Because of the inherent chirality of DNA, its interaction with chiral ligands should give rise to distinguishable diastereomers. Such a chiral discrimination is interesting as it could provide insight about mechanisms of interactions and, more specifically, stereoselective effects that might be exploited for nucleic acid target recognitions. While the attempts over the years to achieve enantioselective binding of propeller-shaped transition metal complexes have been generally rather unimportant as to discriminating power,[12] the introduction of cyclohexyl residues in the backbone of a peptide nucleic acid (PNA) has recently been found to result in strong discrimination between the (*R,R*)- and (*S,S*)-enantiomers in mixed sequence PNA−DNA duplexes.[13] Enantioselectivity could be expected to be most pronounced for interactions with the helical grooves of DNA, while the insertion of chiral compounds between the achiral DNA bases by way of intercalation is generally believed to give less enantioselectivity.

In a previous study, we found that piperazinecarbonyloxyethyl-substituted anthracenes and pyrene **1a**−**c** intercalate with their aromatic part between the DNA bases, while the ionic tail is pulled into the minor groove by electrostatic attraction.[1] Compounds **1a** and **1b** were found to have a significant preference for AT, interpreted in terms of steric hindrance in the minor groove of GC which due to the exocyclic amino groups of guanine could not accommodate the piperazinium tail.

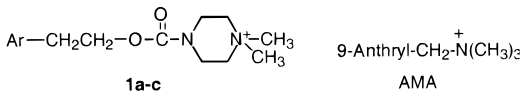

1a-c AMA

a: Ar=9-anthryl; **b**: Ar=1-pyrenyl; **c**: Ar=9-(10-phenyl)anthryl

(1) Becker, H.-C.; Nordén, B. *J. Am. Chem. Soc.* **1999**, *121*, 11947−11952.
(2) Kumar, C. V.; Asuncion, E. H. *J. Am. Chem. Soc.* **1993**, *115*, 8547−8553.
(3) Miller, K. J.; Newlin, D. D. *Biopolymers* **1982**, *21*, 633−652.
(4) Strekowski, L.; Wilson, W. D.; Mokrosz, J. L.; Mokrosz, M. J.; Harden, D. B.; Tanious, F. A.; Wydra, R. L.; Crow, S. A. J. *J. Med. Chem.* **1991**, *34*, 580−588.
(5) Wilson, W. D.; Wang, Y.-H.; Kusuma, S.; Chandrasekaran, S.; Yang, N. C.; Boykin, D. W. *J. Am. Chem. Soc.* **1985**, *107*, 4989−4995.
(6) Müller, W.; Crothers, D. M. *Eur. J. Biochem.* **1975**, *54*, 267−277.
(7) Müller, W.; Crothers, D. M. *Eur. J. Biochem.* **1975**, *54*, 279−291.
(8) Ren, J.; Chaires, J. B. *Biochemistry* **1999**, *38*, 16067−16075.
(9) Atwell, G. J.; Baguley, B. C.; Denny, W. A. *J. Med. Chem.* **1988**, *31*, 774−779.
(10) Atwell, G. J.; Bos, C. D.; Baguley, B. C.; Denny, W. A. *J. Med. Chem.* **1988**, *31*, 1048−1052.
(11) Bailly, C.; Waring, M. J. *Biochemistry* **1993**, *32*, 5985−5993.
(12) Nordén, B.; Lincoln, P.; Åkerman, B.; Tuite, E. *DNA Interactions with Substitution-Inert Transition Metal Ion Complexes*; Sigel, A., Sigel, H., Eds.; Marcel Dekker: New York, 1996; Vol. 33, pp 177−252.
(13) Lagriffoule, P.; Wittung, P.; Eriksson, M.; Jensen, K. K.; Nordén, B.; Buchardt, O.; Nielsen, P. E. *Chem. Eur. J.* **1997**, *4*, 912−919.

10.1021/ja000464x CCC: $19.00
Published on Web 08/18/2000

Table 1. Binding Constants and Binding Site Widths As Determined from McGhee−von Hippel Analysis of Absorbance Titrations

	poly(dA-dT)$_{2)}$		poly(dG-dC)$_{2)}$	
compd	K/M^{-1}	n/bp	K/M^{-1}	n/bp
1a	$4 \pm 1 \times 10^5$	2.3 ± 0.3	$3 \pm 1 \times 10^4$	2.1 ± 0.1
AMA	$2 \pm 1 \times 10^5$	2.0 ± 0.3	$3 \pm 1 \times 10^5$	2.3 ± 0.3
(*S*)-**2**	$2 \pm 1 \times 10^4$	2 ± 0.3	$3 \pm 2 \times 10^3$	2, $\omega \approx 30$
(*R*)-**2**	$1 \pm 0.5 \times 10^4$	2 ± 0.3	$2 \pm 1 \times 10^3$	2, $\omega \approx 60$
1b	$2 \pm 0.5 \times 10^6$	2.6 ± 0.3	ca. 10^5	2−3
(*R*)-**3**	$4 \pm 2 \times 10^5$	2 ± 0.3	$1 \pm 0.5 \times 10^4$	2.0 ± 0.3
(*S*)-**3**	$5 \pm 4 \times 10^5$	2 ± 0.3	ca. 10^4	ca. 2

The minor groove of AT, however, provides space enough, thereby permitting the aromatic moiety to intercalate deep into the DNA. It was further concluded that the ethyloxycarbonylpiperazinium tail does not interfere significantly with the minor groove of AT, as the binding strength of **1a** to AT is the same as that of anthracene model (9-anthrylmethyl)trimethylammonium iodide (AMA). The 10-phenyl group of **1c**, being orthogonal to the anthracene plane, was found to prevent intercalation because of interference with the exterior of the DNA.

To gain a better understanding of the origin of the sequence specificity found for **1**, we extended the investigation to the α-methyl-substituted analogues **2**−**4**. The binding modes of **2**−**4**

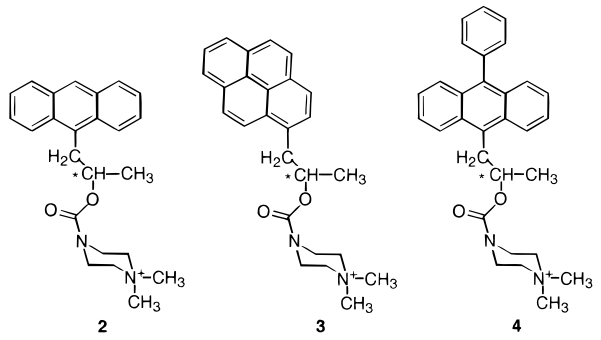

should in principle parallel those of **1**. In addition, the increased steric demand of the tail moiety due to the α-methyl group could further enhance the sequence specificity. Finally, compounds **2**−**4** are of interest because of their chirality, which could result in enantiomeric differentiation upon interaction with DNA. For that reason, we chose to prepare the optically active forms of **2**−**4**.

Experimental Section

Syntheses. The preparation of racemic α-methyl(9-anthryl)ethanol and subsequent chromatographic separation of enantiomers has been described earlier.[14] We here report the preparation of the optically active chloroformates. For the syntheses of **5**, **6**, and **7**, one example each is described in detail. All analogous compounds listed below were prepared in the same fashion. Flash chromatographic purifications involved a 3.5 cm × 35 cm column. Melting points were taken on a hot-stage microscope and are uncorrected. ^{1}H NMR spectra were taken in $CDCl_3$ solution on a Varian 400 MHz instrument, with chemical shifts given in parts per million downfield from Me_4Si. Circular dichroism spectroscopy was used to verify the enantiomeric purity (Table 1, Supporting Information).

Reaction of 9-Bromoanthracene with Optically Active 1,2-Epoxypropane To Give Optically Active α-Methyl-9-anthraceneethanol (5a). 9-Anthryllithium was prepared by adding *n*-butyllithium (4 mL of a 2.5 M solution in hexanes) to an ice-cooled stirred solution of 9-bromoanthracene (2.57 g; 10 mmol) in ether (150 mL) and stirring the yellow suspension for 1 h. To this suspension was then added a solution of optically active propylene oxide (1 mL) in ether (3 mL). The reaction mixture was stirred for 1 h at ice-bath temperature and subsequently for 2 h at room temperature. Workup involved addition of saturated aqueous ammonium chloride solution (100 mL) and ether (100 mL), separation of the organic layer, and drying over sodium sulfate. Vacuum evaporation of solvent gave a pale yellow crystalline residue. Flash column chromatography (silica gel/dichloromethane) gave 1.48 g (44%) of **5a** as pale greenish yellow needle-shaped crystals with bluish fluorescence, mp 125−126 °C. ^{1}H NMR δ 8.38 (s, H-10), 8.32 (d, J = 8 Hz, 2), 8.0 (d, J = 9 Hz, 2), 7.49 (m, 4), 4.34 (m, methine), 3.80 (m, methylene), 1.41 (d, J = 6 Hz, methyl), OH (broad, hidden).

α-Methyl-1-pyreneethanol (5b): Fluffy colorless needle-shaped crystals, mp 115−116 °C. ^{1}H NMR δ 8.3−7.8 (9, arom H), 4.30 (m, methine), 3.50 (m, methylene), 1.37 (d, J = 7 Hz, methyl), OH (broad, hidden).

α-Methyl(10-phenyl-9-anthracene)ethanol (5c): Yellow needles, mp 135−137 °C. ^{1}H NMR δ 8.40 (d, J = 9 Hz, 2), 7.68 (d, J = 9 Hz, 2), 7.56−7.35 (9), 4.44 (m, methine), 3.91 (dd, J = 14, 8 Hz, 1), 3.87 (dd, J = 14, 5 Hz, 1), 1.49 (d, J = 6 Hz, methyl), OH (broad, hidden).

Reaction of Phosgene with Optically Active α-Methyl-9-anthraceneethanol (5a) To Give Optically Active α-Methyl(9-anthryl)-ethylchloroformate (6a). Pyridine (0.5 mL) was added to a stirred ice-cooled solution of phosgene in toluene (15 mL; 20%) to give a pale yellow precipitate. Stirring at icebath temperature was continued for 10 min. To this suspension was then added dropwise over a period of 75 min a solution of **5a** (945 mg; 4 mmol) in ether (60 mL). Suction filtration through Celite of the resulting colorless suspension gave a clear filtrate. Vacuum evaporation of solvent from the filtrate gave a pale yellow oily residue which was dissolved in a little pentane. Colorless crystals precipitated from the solution upon brief storage at freezer temperature. Suction filtration gave 960 mg (80%) of **6a**, mp 65−66 °C. ^{1}H NMR δ 8.40 (s, H-10), 8.30 (d, J = 9 Hz, 2), 8.02 (d, J = 10 Hz, 2), 7.59−7.44 (4), 5.46 (m, methine), 4.12 (dd, J = 14, 6.4 Hz, 1), 3.91 (dd, J = 14.3, 6.4 Hz, 1), 1.37 (d, J = 6.3 Hz, methyl).

α-Methyl(1-pyrenyl)ethyl chloroformate (6b): Colorless crystals, mp 69−71 °C. ^{1}H NMR δ 8.3−7.84 (9, arom H), 5.43 (m, methine), 3.80 (dd, J = 14, 6.3 Hz, 1), 3.50 (dd, J = 14, 7.4 Hz, 1), 1.41 (d, J = 6.3 Hz, methyl).

α-Methyl(10-phenyl-9-anthryl)ethyl chloroformate (6c): Colorless crystals, mp 84−85 °C. ^{1}H NMR δ 8.34 (d, J = 9 Hz, 2), 7.68 (d, J = 9 Hz, 2), 7.56−7.39 (9), 5.54 (m, methine), 4.19 (dd, J = 14, 6 Hz, 1), 4.02 (dd, J = 14, 8 Hz, 1), 1.44 (d, J = 6 Hz, methyl).

Reaction of 6a with 1-Methylpiperazine To Give the α-Methyl-(9-anthryl)ethyl Ester of 4-Methylpiperazinecarboxylic Acid (7a). A solution of **6a** (300 mg; 1 mmol) in dry THF (2 mL) was added to a stirred solution of 1-methylpiperazine (0.5 mL; 4.5 mmol) in dry THF (10 mL) to immediately give a colorless crystalline precipitate. Stirring was continued for 1 h, whereafter the precipitate was removed by suction filtration. Vacuum evaporation of solvent gave a colorless oily residue, which was dissolved in 20 mL of ether. Workup consisted of washing the solution three times with 20 mL of water and drying the organic phase with sodium sulfate. Vacuum evaporation of solvent afforded an oily residue, which crystallized on treatment with a little dichloromethane and petroleum ether. Suction filtration gave 350 mg (96%) of **7a** as pale yellow needles, mp 89 °C. ^{1}H NMR δ 8.44 (d, J = 8.8 Hz, 2), 8.38 (s, H-10), 8.0 (d, J = 8 Hz, 2), 7.53−7.46 (4), 5.32 (m, methine), 4.07 (dd, J = 14, 7.2 Hz, 1), 3.80(dd, J = 14, 7.6 Hz, 1), 3.37 (s, broad, 4, piperazine), 2.33 (s, broad, 2, piperazine), 2.24 (s, 3, N-CH_3), 2.05 (s, broad, 2, piperazine), 1.30 (d, J = 6.4 Hz, α-methyl).

α-Methyl(1-pyrenyl)ethyl Ester of 4-Methylpiperazinecarboxylic Acid (7b). The reaction of **6b** with 1-methylpiperazine was carried out in the same fashion as described for the preceding experiment. Colorless oil. ^{1}H NMR δ 8.47 (d, J = 9 Hz, 1), 8.18−7.88 (8), 5.32 (m, 1, methine), 3.84 (dd, J = 14, 6.4 Hz, 1), 3.43 (s, broad, 4, piperazine), 3.40 (dd, J = 14, 7.2 Hz, 1), 2.33 (s, broad, 2, piperazine), 2.21 (s, 3, N-CH_3), 1.30 (d, J = 6.4 Hz, α-methyl).

α-Methyl(10-phenyl-9-anthryl)ethyl Ester of 4-Methylpiperazinecarboxylic Acid (7c). The preparation of **7c** proceeded in the same fashion as described for **7a**. Pale yellow oil. ^{1}H NMR δ 8.50 (d,

(14) Thorsén, G.; Engström, A.; Josefsson, B. *J. Chromatogr., A* **1997**, *786*, 347−354.

J = 9 Hz, 2), 7.65 (d, J = 9 Hz, 2), 7.54−7.33 (9, aromatic), 5.38 (m, methine), 4.13 (dd, J = 14, 7 Hz, 1), 3.87 (dd, J = 14, 7 Hz, 1), 3.39 (s, broad, 4, piperazine), 2.34 (s, broad, 2, piperazine), 2.24 (s, N-CH_3), 2.0 (s, broad, 2, piperazine), 1.37 (d, J = 6 Hz, α-methyl).

Quaternary salts 2−4 were prepared by stirring overnight a solution of the corresponding derivative **7** in acetonitrile with an excess of methyl iodide. Evaporation of solvent and subsequent treatment of the residue with dichloromethane and ether afforded **2−4** as crystalline material. **2**: Pale yellow small needles, mp 138−140 °C. **3**: Colorless flakes, mp 168−170 °C. **4**: Pale yellow small needles, mp 198−200 °C. Positive ion FAB mass spectrometry yielded the following masses: **2**, 377.221 (calcd 377.223); **3**, 401.226 (calcd 401.223); **4**, 453.254 (calcd 453.257).

Materials and Methods. Calf thymus DNA (Sigma) and synthetic polynucleotides $[Poly(dA\text{-}dT)]_2$ (AT) and $[Poly(dG\text{-}dC)]_2$ (GC) (Pharmacia) were used without further purification. All experiments were conducted at 20 °C in pH 7.2 buffer (1 mM sodium cacodylate, 5 mM Tris, 10 mM NaCl). Absorbance titrations were carried out on a Cary 4B spectrophotometer by adding small aliquots of DNA to a solution of ligand, the dilution taken into account in the evaluation. Titrations of enantiomers were performed with the absorbances matched within 1%. Due to the low binding constants it was impossible to directly obtain the spectra of the bound compounds. The spectra of the bound ligands were constructed by subtraction of the spectrum of the free compound multiplied by an appropriate weight factor. The correct weight factor was determined by visual inspection of the resulting bound spectrum, and by comparison with LD spectra. Flow LD was measured on Jasco J-500A and J-720A spectropolarimeters equipped with Oxley prisms for LD operation. The reduced dichroism (LD^r) was formed as LD/A^{iso}, where A^{iso} constitutes the isotropic absorbance of the bound compound.[15,16] Binding isotherms were evaluated by the method of McGhee and von Hippel, taking cooperativity into account only when the noncooperative fit was unacceptable.[17,18] Binding enthalpies and entropies were determined from van't Hoff plots, with binding constants calculated as described above. Salt dependencies of the binding constants were determined at 20 °C. A division of the total binding free energy $\Delta G°$ into a polyelectrolyte ($\Delta G_{pe} = -RT \ln[Na^+](\partial \ln K/\partial \ln[Na^+])$) and a nonpolyelectrolyte ($\Delta G_{nonpe} = \Delta G° - \Delta G_{pe}$) part was done as described previously.[19,20] The contribution to the entropy of binding from the counterion release was calculated as $\Delta S_{Na^+} = R \ln[Na^+](\partial \ln K/\partial \ln[Na^+])$.[21,22] Molecular models were made using the AMBER (DNA) and MM+ (ligand) force fields as implemented in the HyperChem program.

Results

Electronic Spectra. Absorption spectra of compounds **2−4**, as well as of their complexes with AT and GC, are shown in Figure 1. Addition of calf thymus DNA or synthetic polynucleotides to solutions of the (*R*)- and (*S*)-enantiomers of **2−3** leads to red-shift and strong hypochromicity (>50%) in the anthracene and pyrene absorption bands, indicating strong interaction with the nucleobases. The absorbance titrations (Figure 1, Supporting Information) of both enantiomers of **2** and **3** with AT and GC exhibit isosbestic points, the presence of which we take as a justification to use a two-state model for the binding process.

Circular Dichroism. The intrinsic CD of the anthracene and pyrene chromophores of **2−4** dominates completely over any induced CD in the complexes, leading to unchanged CD signs throughout the titration (Figure 2, Supporting Information).

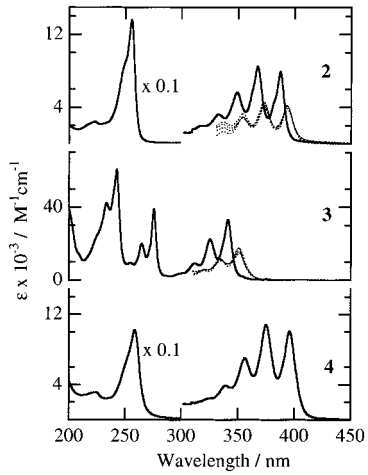

Figure 1. Absorption spectra of free (solid lines) **2−4** and AT and GC complexes (dotted lines) of (*R*)- and (*S*)-**2** and **3**. Note that for both (*R*)- and (*S*)-**2** and **3**, the spectra of the compounds bound to AT and GC are virtually identical.

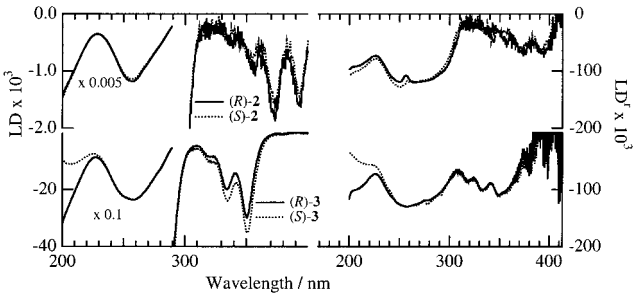

Figure 2. Linear dichroism (left panel) and reduced dichroism (right panel) of the DNA complexes of (*R*)- and (*S*)-**2** and **3**.

Linear Dichroism. The DNA complexes of (*R*)- and (*S*)-enantiomers of **2** and **3** show negative LD in the ligand absorption region, indicating intercalative binding (see Figure 2). To investigate the binding in detail, we measured LD spectra of the (*R*)- and (*S*)-enantiomers of **2** and **3** bound to AT and GC. As observed for the complexes with calf thymus DNA, there is no distinction between the (*R*)- and (*S*)-enantiomers. For the GC complexes of (*R*)-**2** and (*S*)-**2**, both enantiomers show at the experimental conditions negligible LD (Figure 3, Supporting Information). Analogously with the behavior of the previously investigated achiral 9-(10-phenyl)anthracene **1c**, both enantiomers of the phenyl-substituted anthracene **4** are characterized by complete lack of LD in the anthracene absorption region.

Binding Isotherms. Binding parameters are collected in Table 1 and Figure 4, Supporting Information. It may be argued that polynucleotides such as AT and GC are not very good models for mixed-sequence DNA, but based on the results obtained for the achiral ligands **1** and AMA, we believe that the results obtained may be of importance for the design of sequence-specific intercalators. Because of the low affinities for AT and GC, the titrations were carried out over a limited set of binding ratios. Nevertheless, the data should give a good indication of affinities for AT and GC. Except for the binding of (*R*)-**2** and (*S*)-**2** to GC, the binding of **2** and **3** to AT and GC can be described by a noncooperative McGhee−von Hippel model. It was necessary to include cooperativity ($\omega > 1$) to accurately describe the binding of (*R*)-**2** and (*S*)-**2** to GC. Because of the lack of isosbestic points in the absorbance titrations of (*R*)-**4** and (*S*)-**4** to AT, a two-state model cannot be applied for this compound. As for the binding of (*R*)-**4** and (*S*)-**4**

(15) Nordén, B.; Kubista, M.; Kurucsev, T. *Q. Rev. Biophys.* **1992**, *25*, 51−170.
(16) Nordén, B. *Appl. Spectrosc. Rev.* **1978**, *14*, 157−248.
(17) McGhee, J. D.; von Hippel, P. H. *J. Mol. Biol.* **1974**, *86*, 469−489.
(18) McGhee, J. D.; von Hippel, P. H. *J. Mol. Biol.* **1976**, *103*, 679.
(19) Chaires, J. B.; Satyanarayana, S.; Suh, D.; Fokt, I.; Przewloka, T.; Priebe, W. *Biochemistry* **1996**, *35*, 2047−2053.
(20) Chaires, J. B.; Priebe, W.; Graves, D. E.; Burke, T. G. *J. Am. Chem. Soc.* **1993**, *115*, 5360−5364.
(21) Wilson, W. D.; Lopp, I. G. *Biopolymers* **1979**, *18*, 3025−3041.
(22) Hopkins, H. P.; Wilson, W. D. *Biopolymers* **1987**, *26*, 1347−1355.

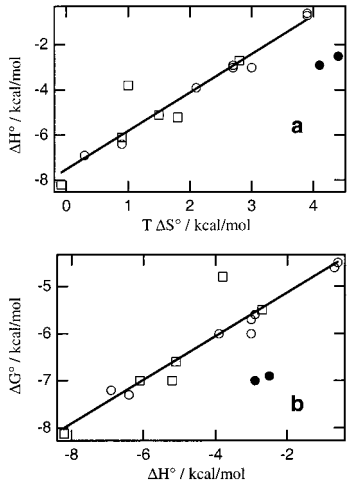

Figure 3. Enthalpy−entropy compensation in the DNA binding of achiral and chiral ligands **1** and **2**. Unfilled circles indicate data for compounds **2** and **3**, squares indicate data for compounds **1a**−**c**, and filled circles indicate data for AMA.

to GC, the binding is relatively weak, and we were unable to extract an end-point spectrum, but could estimate the affinity for GC to be about 10^3 M^{-1}.

Thermodynamic Properties. The thermodynamic parameters for the binding of both enantiomers of **2** and **3** to AT and GC are summarized in Table 2 and Figure 5, Supporting Information. All binding enthalpies are negative, and all binding entropies positive. As expected from the binding data, there are virtually no differences between enantiomers. However, there is a remarkable difference between the AT and GC complexes in the relative contributions of $\Delta H°$ and $T\Delta S°$ to the binding free energy. The reduced affinity for GC observed for **2** and **3** is reflected in a significantly smaller ratio $-\Delta H°/T\Delta S°$ compared to the binding to AT.

Discussion

Spectra. The substantial red-shifts and hypochromicities seen in the absorption of **2** and **3** upon binding to DNA spectra show that the anthracene and pyrene chromophores interact strongly with the nucleobases. This observation, together with the negative LD, indicates an intercalative binding mode. The very weak LD displayed by the GC complexes of the (*R*)- and (*S*)-enantiomers of **2** and **3** is likely the result of partial intercalation. In this binding mode, the aromatic moiety is not locked firmly at an angle of 90° to the helix axis, but occupies a distribution of orientations around 90°. Since any orientation different from 90° to the helix axis will give a positive contribution to the LD, the overall magnitude of LD and LD^r is reduced. This is consistent with the binding mode concluded for the GC complexes of achiral analogues **1a** and **1b**. The difference between enantiomers in the absorbance titrations can be attributed to different affinities of the (*R*)- and (*S*)-enantiomers for DNA. As shown in Table 2, the (*S*)-enantiomers of both **2** and **3** bind stronger to DNA than the corresponding (*R*)-enantiomers. The lack of LD in the DNA complexes of (*R*)-**4** and (*S*)-**4** suggests an external binding mode, similar to what was concluded for the achiral analogue **1c**. In the CD spectra, the main features of DNA-bound **2** and **3** are those of the free ligands. For (*R*)- and (*S*)-**2**, however, there is a deviation from mirror symmetry at the red end of the spectrum, with the CD for both enantiomers pulling toward positive values. This is probably an effect of a positive induced CD, and from the identical sign of the induced CD for both enantiomers similar intercalation geometries seem likely.[23,24]

Binding Constants. Although the data presented here do not per se rule out intercalation from the major groove, the following arguments speak in favor of binding from the minor groove. In AT, the major groove contains the exocyclic amino and methyl groups of adenine and thymine, while the minor groove is comparably less congested, and, in addition, has a more negative electrostatic potential. In GC, both grooves contain groups that may obstruct binding. Since we observe significantly stronger binding to AT than to GC for achiral compounds **1** as well as chiral compounds **2**−**3**, but not for model anthracene AMA, we believe that intercalation from the minor groove is the most likely binding mode for **1**−**3**. Indeed, molecular models using the AMBER force field suggest that **2** and **3** can intercalate from the minor groove, while keeping the piperazinium bound in the groove itself (Figure 4). Furthermore, the models confirm the hypothesis (see below) that, for each enantiomer, there are two possible binding geometries: one in which the piperazinium is pointing "upwards" (with respect to the intercalating moiety) in the minor groove, and one in which the piperazinium points "downwards".

As can be seen in Table 3, the presence of the α-methyl group lowers the affinity of **2**−**3** for both AT and GC by 1 order of magnitude. We believe that this is due to clashing of the methyl group with the outer parts of the DNA. The reduced affinity is interesting in view of that the piperazinecarbonyloxyethyl substituent in **1** does not affect the binding to AT, but only the affinity for GC. The effect of the methyl group corroborates the binding mode proposed for achiral ligands **1**: in AT, the piperazinium tail fits snugly into the minor groove, but steric hindrance prevents its efficient binding to GC. Thus, for both enantiomers of **2** and **3** the effect of the α-methyl group appears to be mainly to reduce the binding strength by steric repulsion. In line with this argument is the absence of LD for the GC complexes of (*R*)- and (*S*)-enantiomers of **2** and **3**. It indicates that here the intercalating moiety is only loosely bound, and has access to a large conformational space, which leads to the observed near random orientation.

Chiral Discrimination. The observed difference in binding constant between the two enantiomers is small. This is remarkable in view of the pronounced effect of the methyl group on the binding constant, which suggests that the methyl group does indeed interact significantly with the DNA. Since the methyl goup is separated from the intercalator by only one methylene link, it is likely to be in a chiral environment formed by the helical rise of stacked nucleobases. A possible explanation for the absence of chiral discrimination can be the lack of orientation polarity in the binding, as illustrated in Figure 4, in which we have used simple molecular modeling to investigate the binding. The binding is characterized by the following features (see Figure 4).

1. In the intercalator−DNA complex, depending on the handedness of the ligand, the α-methyl group is directed either *away from* or *toward* the DNA, leading to less or more interference, respectively.

2. The intercalating moiety binds equally well with the piperazinium tail "up" and "down" with respect to the DNA helix axis.

3. Rotating the ligand 180° around the base pair short-axis, thus changing the position of the piperazinium from *above* to

(23) Rodger, A.; Nordén, B. *Circular Dichroism and Linear Dichroism*; Oxford University Press: Oxford, 1997.

(24) Lyng, R.; Rodger, A.; Nordén, B. *Biopolymers* **1991**, *31*, 1709−1820.

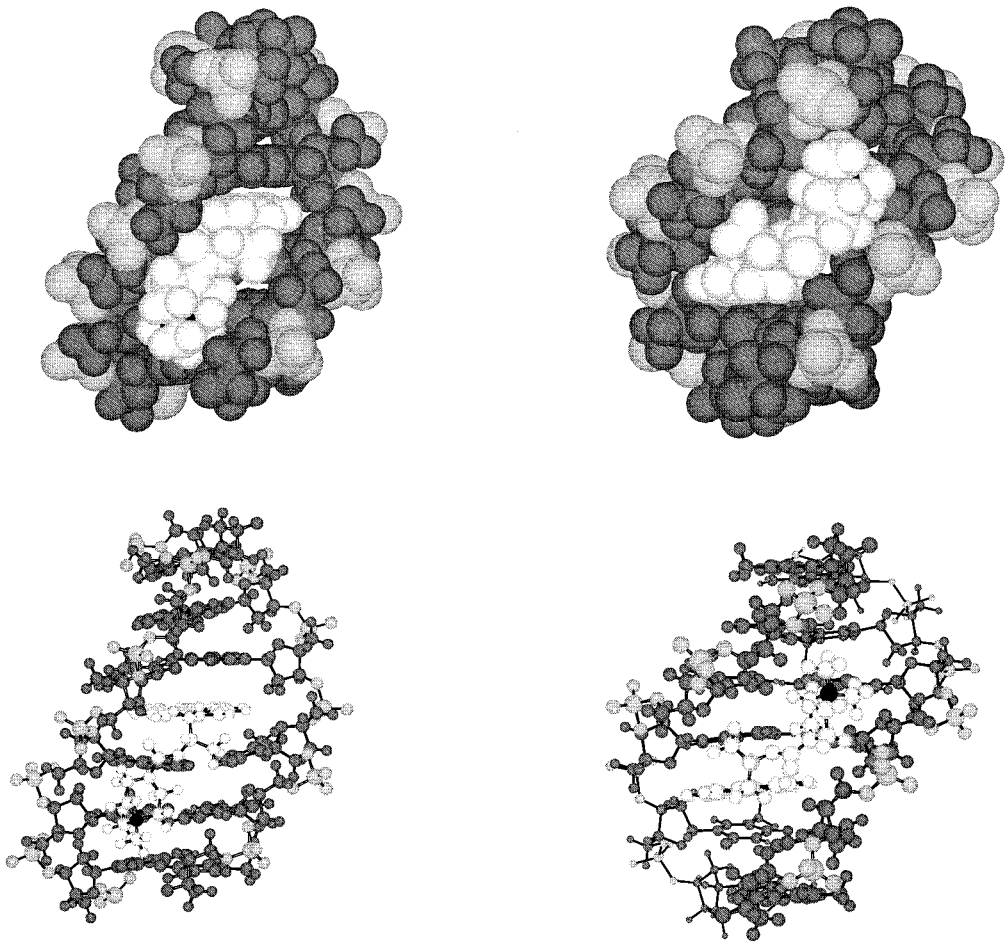

Figure 4. AMBER/MM+ models of (*R*)-**3** bound to AT. Left panels: piperazinium tail "downwards". Right panels: piperazinium tail "upwards". The models have been color-coded using the following scheme: **3**, light gray; DNA phosphate groups, medium gray; DNA backbone and bases, dark gray; piperazinium nitrogen, black.

Table 2. Thermodynamic Parameters[a] for the Binding of (*R*)- and (*S*)-**2** and **3** to AT and GC (Uncertainties in $\Delta H°$ and $T\Delta S°$ Are Estimated To Be Less than 0.5 kcal/mol)

complex	$\Delta G°$	$\Delta H°$	$-T\Delta S°$	ΔG_{pe}	ΔG_{non-pe}	$-T\Delta S_{non-pe}$	s^b
(*R*)-**2**:AT	−5.6	−2.9	−2.7	−3.3	−2.3	+0.6	−1.2
(*S*)-**2**:AT	−5.7	−3.0	−2.7	−3.3	−2.4	+0.6	−1.2
(*R*)-**2**:GC	−4.5	−0.6	−3.9	−1.9	−2.6	−2.1	−0.7
(*S*)-**2**:GC	−4.6	−0.7	−3.9	−1.9	−2.7	−2.1	−0.7
(*R*)-**3**:AT	−7.2	−6.9	−0.3	−2.2	−5.0	+1.8	−0.8
(*S*)-**3**:AT	−7.3	−6.4	−0.9	−2.2	−5.1	+1.2	−0.8
(*R*)-**3**:GC	−6.0	−3.9	−2.1	−2.6	−3.4	+0.6	−1.0
(*S*)-**3**:GC	−6.0	−3.0	−3.0	−2.6	−3.4	−0.3	−1.0

[a] All values are in kcal/mol at 20 °C for 10 mM NaCl ionic strength. [b] $\partial \ln K/\partial \ln [Na^+]$.

Table 3. Qualitative Comparison of Affinities (in M^{-1}) for AT and GC of Achiral Ligands **1** and Chiral Ligands **2**−**3**

intercalator	substituent	K_{AT}	K_{GC}
9-anthryl	$-CH_2N(CH_3)_3$	10^5	10^5
9-anthryl	$-CH_2CH_2$-O-CO-piperazinium	10^5	10^4
9-anthryl	$-CH_2CH(CH_3)$-O-CO-piperazinium	10^4	10^4
1-pyrenyl	$-CH_2CH_2$-O-CO-piperazinium	10^6	10^5
1-pyrenyl	$-CH_2CH(CH_3)$-O-CO-piperazinium	10^5	10^4

below the intercalating moiety, changes for each enantiomer the position of the methyl group from *away* to *toward* (or vice versa), and may thus change the enantioselection.

As a result, although for each orientation there may be significant chiral discrimination, this is on average *canceled* because of lack of polarity in the intercalative binding, that is, the enantiomer that is favored when the tail is directed "up" is disfavored when the tail is directed "down", and vice versa

Thermodynamics. From the spectroscopic observations we have inferred that the binding of *(R)*- and *(S)*-**2** and **3** to AT involves tighter binding than to GC. This notion is supported by the thermodynamic data obtained from van't Hoff plots. For both enantiomers of **2** and **3**, the enthalpy of binding for the AT complexes is significantly more negative than that for the GC complexes. We believe that the exothermic binding has its origin in both hydrophobic and electrostatic interactions. Thus, the higher exothermicity for the AT binding can be interpreted as spatially tighter binding, involving deep intercalation and significant van der Waals interaction of intercalator with the nucleobases. This is in line with the conclusions from the polarization spectra, which suggest that the compounds **1**−**3** intercalate less deeply into GC than into AT.

It seems that the enthalpy−entropy compensation observed for the DNA binding of compounds **1** and **2** is of a similar nature. If one plots $\Delta H°$ vs $T\Delta S°$ (Figure 3a) and $\Delta G°$ vs $\Delta H°$ (Figure 3b), the data for the AT and GC complexes of **1a**−**c** and **2**−**3** fall on a straight line, which is indicative of enthalpy−entropy compensation.[25−27] The observation that the achiral compounds **1** and their chiral analogues **2**−**3** have similar

(25) Gilli, P.; Ferretti, V.; Gilli, G.; Borea, P. A. *J. Phys. Chem.* **1994**, *98*, 1515−1518.
(26) Krug, R. R.; Hunter, W. G.; Grieger, R. A. *J. Phys. Chem.* **1976**, *80*, 2335−2341.
(27) Krug, R. R.; Hunter, W. G.; Grieger, R. A. *J. Phys. Chem.* **1976**, *80*, 2341−2351.

binding thermodynamics with respect to enthalpy−entropy compensation supports the proposed similarities in the binding mode. Furthermore, the correlation of binding exothermicity with binding constant is in good agreement with the data obtained from the LD spectroscopic data: tight binding to AT and loose binding to GC.

The observed salt dependencies of the binding constants are overall somewhat smaller than expected. For a monovalent DNA intercalator, the slope $\partial \ln K/\partial \ln[Na^+]$ is expected to be about −1.2, and for an uncharged intercalator about −0.2.[19,20,28−31] Possible explanations for the smaller slopes (0.7−1.2) observed for the binding of (*R*)- and (*S*)-**2** and **3** to AT and GC include differences between the alternating copolymer and mixed-sequence DNA, and that the interaction of **2** and **3** with DNA is not that of a "true" intercalator, but rather that of a combination of intercalation and external binding.

Conclusions

1. Both enantiomers of anthracene derivative **2** and pyrene derivative **3** are found to intercalate into both alternating AT and GC contexts.

2. The α-methyl substituent of compounds **2**−**4** does not significantly change the effective binding geometry compared to that of the achiral analogues **1a**−**c**, despite that the affinity for both AT and GC sequences is reduced because of increased steric interference.

3. The binding of the (*S*)-enantiomers of **2** and **3** to AT is favored. The enantioselectivity is small, which may be attributed to a lack of polarity for the intercalative part of the binding. The steric interference of the methyl group in the (*R*)- and (*S*)-enantiomers is similar if one of the ligands is rotated 180° with respect to the base pair short-axis.

4. The strong sequence specificity is also reflected by a pronounced enthalpy−entropy compensation, with the binding to AT involving a much larger ratio $-\Delta H°/T\Delta S°$ than the binding to GC. Thus, the tight binding to AT involves a more favorable enthalpy change and less favorable entropy change than the loose binding to GC.

Supporting Information Available: Molar extinction coefficients and molar circular dichroism for compounds **2**−**7**, absorbance titrations for *(R)*- and *(S)*-**2**−**4** with DNA, CD titrations of **2**−**4** with DNA, LD spectrum of *(R)*- and *(S)*-**3** bound to GC, isotherms for the binding of *(R)*- and *(S)*-**2** and **3** to AT and GC, and van't Hoff plots for the binding of *(R)*- and *(S)*-**2** and **3** to AT and GC (PDF). This material is available free of charge via the Internet at http://pubs.acs.org.

JA000464X

(28) Friedman, R. A. G.; Manning, G. S.; Shahin, M. A. *The Polyelectrolyte Correction to Site Exclusion Numbers in Drug−DNA Binding*; Kallenbach, N. R., Ed.; Adenine Press: Schenectady, NY, 1988; pp 37−65.

(29) Bustamante, C.; Stigter, D. *Biopolymers* **1984**, *23*, 629−645.

(30) Record, M. T., Jr.; Woodbury, C. P.; Lohman, T. M. *Biopolymers* **1976**, *15*, 893−915.

(31) Friedman, R. A. G.; Manning, G. S. *Biopolymers* **1984**, *23*, 2671−2714.